

RESEARCH ARTICLE

Open Access

Adaptation of peroxisome proliferator-activated receptor alpha to hibernation in bats

Yijie Han^{1†}, Guantao Zheng^{1†}, Tianxiao Yang¹, Shuyi Zhang², Dong Dong³ and Yi-Hsuan Pan^{3*}

Abstract

Background: Hibernation is a survival mechanism in the winter for some animals. Fat preserved instead of glucose produced is the primary fuel during winter hibernation of mammals. Many genes involved in lipid metabolism are regulated by the peroxisome proliferator-activated receptor alpha (PPAR α). The role of PPAR α in hibernation of mammals remains largely unknown. Using a multidisciplinary approach, we investigated whether PPAR α is adapted to hibernation in bats.

Results: Evolutionary analyses revealed that the ω value of *Ppara* of the ancestral lineage of hibernating bats in both Yinpterochiroptera and Yangochiroptera was lower than that of non-hibernating bats in Yinpterochiroptera, suggesting that a higher selective pressure acts on *Ppara* in hibernating bats. PPAR α expression was found to be increased at both mRNA and protein levels in distantly related bats (*Rhinolophus ferrumequinum* and *Hipposideros armiger* in Yinpterochiroptera and *Myotis ricketti* in Yangochiroptera) during their torpid episodes. Transcription factors such as FOXL1, NFYA, NFYB, SP1, TBP, and ERG were bioinformatically determined to have a higher binding affinity to the potential regulatory regions of *Ppara* in hibernating than in non-hibernating mammals. Genome-wide bioinformatic analyses of 64 mammalian species showed that PPAR α has more potential target genes and higher binding affinity to these genes in hibernating than in non-hibernating mammals.

Conclusions: We conclude that PPAR α is adapted to hibernation in bats based on the observations that *Ppara* has a more stringent functional constraint in the ancestral lineage of hibernating bats and a higher level of expression in hibernating than in non-hibernating bats. We also conclude that PPAR α plays a very important role in hibernation as hibernators have more PPAR α target genes than non-hibernators, and PPAR α in hibernators has a higher binding affinity for its target genes than in non-hibernators.

Keywords: PPAR α , Hibernation, Bats, Mammals, Molecular evolution, Gene regulation

Background

Hibernation is an adaptive strategy used by some animals to survive cold winter weather when food is scarce [1, 2]. Small mammalian hibernators (e.g., squirrels and bats) undergo a series of torpor-arousal cycles during hibernation, in which a torpor bout lasts for several days or weeks but an arousal bout lasts only several hours [1, 3]. During torpor, the metabolic rate (MR) of these mammals is reduced to 2-4 % of the euthermic metabolism, and their body temperature (T_b) may fall just a few degrees above the ambient temperature; however, both their MR and T_b

are rapidly restored to the euthermic levels upon arousal [2]. The body weight and fat mass of these hibernators are dramatically increased in the pre-hibernation season. The preserved fats are used as the primary energy source during hibernation [2, 4, 5].

Bats belong to the order Chiroptera in the mammalian clade Laurasiatheria [6]. They comprise almost 1-quarter of mammalian species and are the only flying mammals [7, 8]. Hibernating bats (e.g., some species in superfamilies Rhinolophoidea, Emballonuroidea, and Vespertilionoidea) are mostly distributed in subtropical or cold latitudes, whereas non-hibernating bats are mainly reside in warm subtropical or tropical latitudes [9]. Many hibernating bat species in genera *Myotis* and *Rhinolophus* are deep hibernators that stringently control their overall metabolism during torpor [9, 10]. Positive selection in the coding

* Correspondence: yihuanp@gmail.com

[†]Equal contributors

³Laboratory of Molecular Ecology and Evolution, Institute of Estuarine and Coastal Research, East China Normal University, Shanghai 200062, China
Full list of author information is available at the end of the article

regions of some genes, such as *Leptin* and *Bssl*, is found in these bats, suggesting that lipid metabolism has undergone adaptive evolution in response to hibernation [11, 12].

Peroxisome proliferator-activated receptors (PPARs) are nuclear receptors that regulate the expression of many genes (e.g., *Leptin*, *Hmgcs1*, *Ucp1*, and *Pgc1 α*) involved in lipid and glucose homeostasis [13, 14] and the development of obesity, diabetes, and hypertension in mammals [15]. Ligand-dependent transcriptional regulation by PPARs depends on the heterodimerization of PPARs with their coactivators (e.g., RXR). PPARs can also be activated directly in a ligand-independent manner by phosphorylation [16, 17]. 3 different subtypes (α , β , and γ) of PPARs have been identified. PPAR α is activated upon energy deprivation and is highly expressed in the liver, heart, kidney, and adipose tissues [17, 18], while subtypes β and γ , expressed ubiquitously, are associated with cell migration and adipocyte differentiation, respectively [19].

The actions of PPAR α are regulated by the fibroblast growth factor 21 (FGF21), and the PPAR α -FGF21 signaling cascade has been shown to induce torpor in fasting mice [20]. PPAR α is recently shown to shift fuel utilization from carbohydrate to lipid during torpor of arctic ground squirrel, *Urocyon parryi* [21]. A positive selection at the glycine residue of codon 96 (96G) of *Ppara* has been detected in members of super-clade Laurasiatheria (placentals) and suborders of Euarchontoglires (primates and rodents) [22]. In addition, increased expression of PPAR γ and its co-activator PGC-1 α is observed in *Spermophilus tridecemlineatus* squirrels during a cold-induced torpor [23]. The expression of these 2 proteins is also increased in many organs of torpid *Myotis lucifugus* bats [24].

Although differential expression of PPARs and their co-activators (e.g., RXR) has been investigated in some hibernating mammals during different phases of hibernation [21, 23-26], the evolution of PPAR α in hibernating bats remains unknown. Since PPAR α plays a significant role in metabolic regulation during torpor [27], we hypothesize that PPAR α has evolved in bats in adaptation to hibernation. To test this hypothesis, we studied the evolution of *Ppara* in fifty-six species of mammals including twelve species of bats. We also compared mRNA and protein expression of *Ppara* in hibernating bats between torpid and arousal states. The number of potential PPAR α target genes and the binding affinity of PPAR α to these genes in hibernating and non-hibernating bats and other mammalian species were also determined.

Results and Discussion

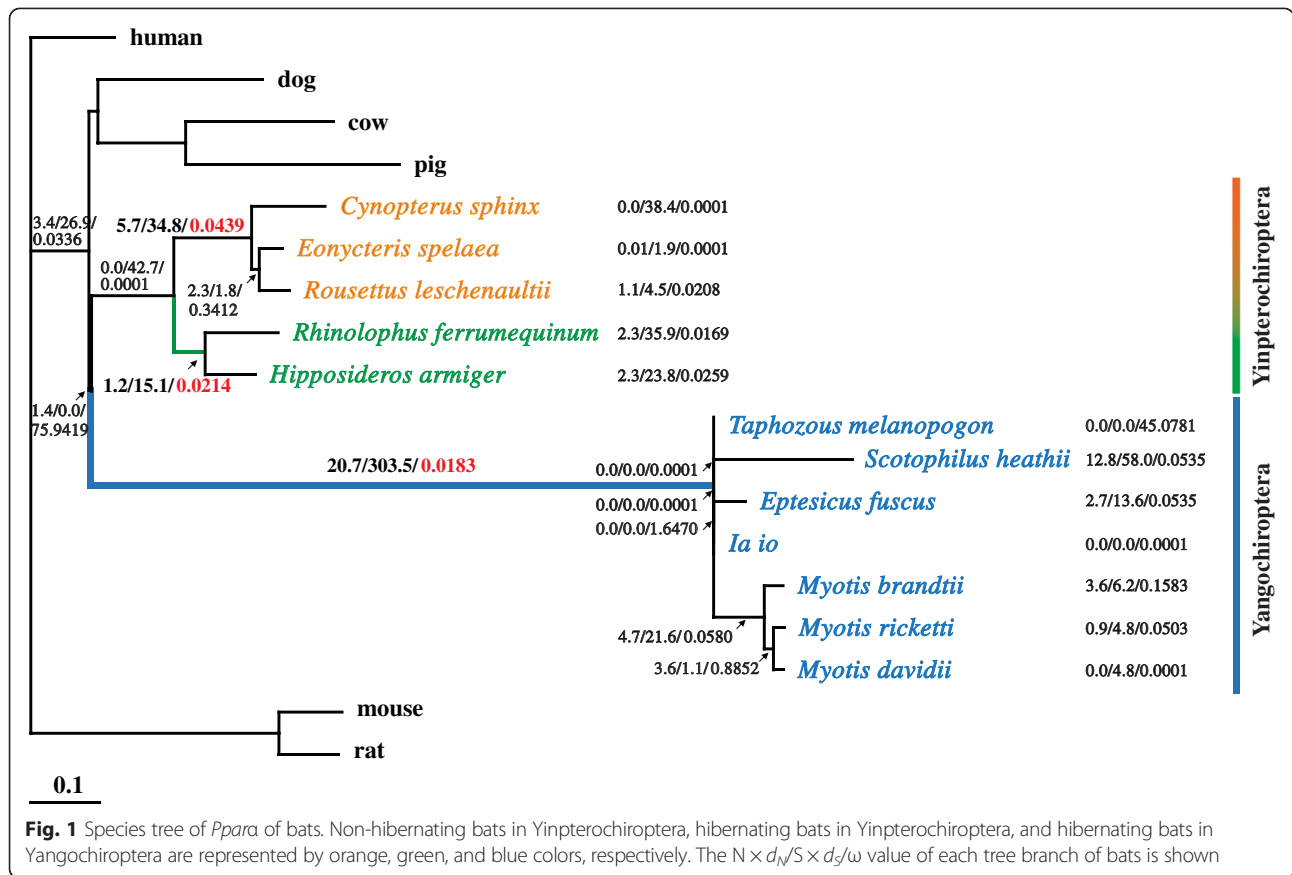
Higher Selection Pressure on *Ppara* in Hibernating Bats

To determine whether the coding region of *Ppara* is positively selected in bats in response to hibernation, we

conducted a branch model test on *Ppara* from 9 hibernating and 3 non-hibernating species of bats by the maximum likelihood method using other mammalian species as an out-group (Fig 1 and Table 1). Although some of the branches were short and might lead to inaccurate estimation of ω (d_N/d_S), the ω value of the ancestral lineage of hibernating bats in both Yinpterochiroptera (Yin) and Yangochiroptera (Yang) was found to be lower than that of non-hibernating bats in Yin (Fig 1), suggesting a higher selective pressure acting on *Ppara* in hibernating bats. A significant lower ω value was obtained by the 2-ratio model E ($P=0.008$) when the ancestral branch of hibernating bats in Yang was labeled for comparison with other branches, indicating that *Ppara* is much more conserved in this lineage (Table 1). It is conceivable that such conservation is required for the survival of hibernating bats, especially for those living in relatively low latitudes (see Additional file 3: Fig S1). No positive selection on any amino acid of *Ppara* was found in the ancestral branches of hibernating bats in both Yin and Yang using the branch-site model A test (see Additional file 1: Table S1 and Additional file 2). There was also no positively selected site detected in these bats using the site model test (see Additional file 1: Table S2 and Additional file 2). However, *Ppara* was found conserved across 56 mammalian species and experienced a higher selective pressure ($\omega=0.057$) in ancestral Chiroptera (see Additional file 1: Table S3, Additional file 2, and Additional file 3: Fig S2). These data suggest that *Ppara* is conserved in evolution and support the previous postulation that heterothermy is an ancestral chiropteran trait [8, 12, 27]. A positive selection on codons 96 and 195 (96G and 195 V) of *Ppara* was detected in these mammals by site model comparisons (M8-M7 model) (see Additional file 1: Table S4 and I file 2). This result is consistent with the positive selection on codon 96 (96G) of PPAR α observed in super-clade Laurasiatheria (placentals) and suborders of Euarchontoglires (primates and rodents) [22].

Upregulation of *Ppara* Expression in Torpid Bats

We next investigated the possibility that bat *Ppara* is adapted to hibernation at the level of transcription. The amount of *Ppara* mRNA in the liver of torpid bats was compared to that of active bats, including the distantly related *Rhinolophus ferrumequinum* and *Hipposideros armiger* bats in Yin and *Myotis ricketti* bats in Yang (Fig 2). Results of quantitative PCR showed that *Ppara* mRNA levels were significantly higher in torpid states than in active states and were increased by 1.19, 1.39, and 1.71 fold in torpid *R. ferrumequinum*, *H. armiger*, and *M. ricketti* bats, respectively (Fig 2). These results indicate that *Ppara* in bats adapts to hibernation at the level of transcription.



The mechanisms for *Ppara* upregulation in torpid bats remain to be investigated. During hibernation, lipid is the main fuel source, and a complex lipid signaling exists not only on the cell membrane but also in the nucleus [28]. Lipid signaling has a close relationship with the signaling pathways of numerous biological processes, such as inflammation, immunity, and glucose and amino acid metabolism [29-32]. PPARs are known to be activated by fatty acids and their derivatives [30, 31]. As some transcription factors may also activate *Ppara* transcription, we used bioinformatic approaches to search

for those that can bind to the 3 potential regulatory regions of *Ppara*, including the region around the transcription start site (TSS_Around), the region upstream from TSS (TSS_Up), and the gene body (TSS_Body) (see Additional file 1: Table S5 and Additional file 2).

We found that transcription factors FOXL1, NFYA, NFYB, SP1, TBP, and ERG can bind to various regulatory regions of *Ppara* in hibernating bats (FOXL1: TSS_Up 10 kb; NFYA, NFYB, and ERG: TSS_Body 7.5 kb; NFYB: TSS_Around 7.5 kb and TSS_Body 5 kb; SP1: TSS_Up 2.5 kb; TBP: TSS_Around 10 kb; ERG:

Table 1 Branch model tests on *Ppara* in bats

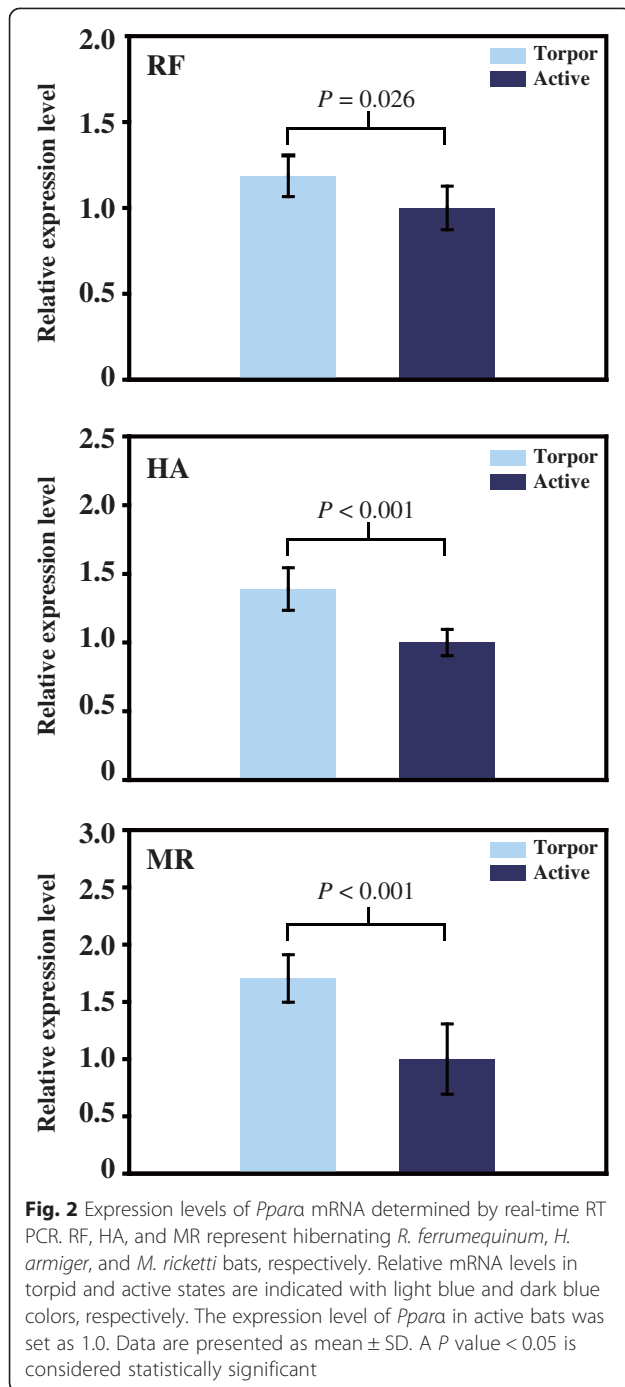
| Model | np ^a | ℓ^b | ω_0^c | $\omega_{\text{labeled}}^d$ | Model compared | $2\Delta\ell$ | P |
|--|-----------------|-----------|--------------|-----------------------------|----------------|---------------|-------|
| A. One ratio: ω_0 | 35 | -5047.902 | 0.033 | ω_0 | | | |
| B. One ratio: $\omega = 1$ (fixed) | 34 | -6001.416 | 1.000 | ω_0 | A and B | 1907.029 | 0.000 |
| C. Free ratio | 67 | -5016.255 | — | — | A and C | 63.294 | 0.001 |
| D. Two ratios: $\omega_0 = \omega_{\text{H-Yan}}, \omega_{\text{H-Yin}}$ | 36 | -5047.813 | 0.033 | 0.021 | A and D | 0.179 | 0.672 |
| E. Two ratios: $\omega_0 = \omega_{\text{H-Yin}}, \omega_{\text{H-Yan}}$ | 36 | -5044.408 | 0.037 | 0.018 | A and E | 6.988 | 0.008 |
| F. Two ratios: $\omega_0, \omega_{\text{HN}}$ | 36 | -5047.801 | 0.032 | 0.0042 | A and F | 0.203 | 0.653 |

^anp: number of parameters.

^b ℓ : $-\ln$ likelihood ratio.

^c ω_0 : one ω ratio for all branches.

^d ω_{labeled} are ω ratios for ancestral branches of Yinpterochiroptera hibernating bats ($\omega_{\text{H-Yin}}$), Yangopterochiropter hibernating bats ($\omega_{\text{H-Yan}}$), and non-hibernating bats (ω_{HN}).



TSS_Body 2.5 kb and 10 kb). In contrast, the NF- κ B p65 subunit (RELA) and E2F1 were found to have the potential to bind to the regulatory regions of *Ppara* in non-hibernating bats (RELA: TSS_Around 7.5 kb; E2F1: TSS_Body 10 kb). FOXL1 is a forkhead box transcription factor and is crucial for liver development and function. Knockdown of *Foxl1* in mice leads to defective intestinal glucose uptake [33]. NFYA, NFYB, and SP1 work cooperatively with PPAR α to regulate the transcription of

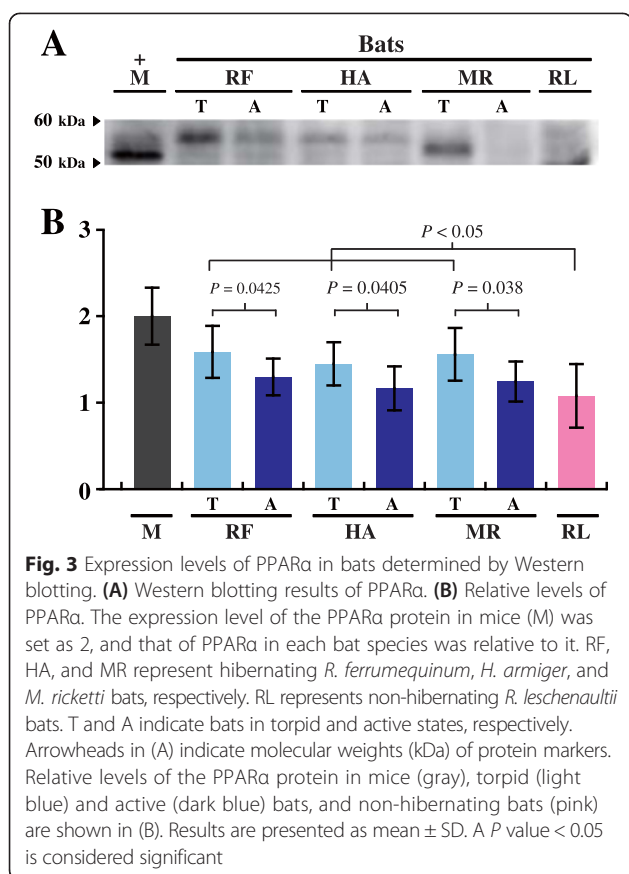
many lipogenic genes [34, 35]. TBP is a TATA box binding protein that interacts with PPAR α to mediate gene transcription [36]. E2F1 regulates the expression of many genes involved in cell cycle control and proliferation [37]. RELA is a pleiotropic TF associated with the regulation of inflammation and immunity. Its activity is repressed by ligand-bound PPARs [37, 38].

It is known that E2F1 competes with histone deacetylase 1 (HDAC1) for binding to SP1 [39]. The activity of HDAC1 is significantly elevated in the skeletal muscle of *Spermophilus tridecemlineatus* ground squirrels during hibernation [40]. In these squirrels, the activation of NF- κ B in skeletal muscle and intestine is positively linked to the antioxidant defense [41, 42]. NF- κ B is also activated in the heart and muscle of torpid *Myotis lucifugus* bats [43]. These observations indicate that NF- κ B and E2F1 are critical for hibernation. Since down regulation of PPAR α depends on an intact signaling pathway of RELA [44] and E2F1 (an endogenous co-activator of NF- κ B) [37], the potential of RELA and E2F1 to bind to the regulatory regions of *Ppara* in non-hibernating bats suggests their roles in transcriptional repression of *Ppara*. Similar binding preferences of FOXL1, NFYA, NFYB, SP1, TBP, ERG, RELA, and E2F1 on *Ppara* were found in many other mammalian species (see Additional file 1: Table S5 and Additional file 2).

Elevated Production of PPAR α in Torpid Bats

To correlate the mRNA level of *Ppara* with its protein level, we determined the amounts of PPAR α protein in mice, hibernating *Rhinolophus ferrumequinum*, *Hipposideros armiger*, and *Myotis ricketti* bats, and non-hibernating *Rousettus leschenaultii* bats by Western blotting. Mouse PPAR α (~55 kDa) protein was used as the positive control (Fig 3A). For each hibernating bat, the amount of PPAR α in the torpid state (T) was compared to that in the active state (A). The levels of PPAR α were found to be increased by 1.22, 1.24, and 1.25 fold in torpid *R. ferrumequinum*, *H. armiger*, and *M. ricketti* bats, respectively ($P < 0.05$) (Fig 3B). These results were consistent with the elevated expression of *Ppara* mRNA in these bats during hibernation (Fig 2).

Because the expression of PPAR α was upregulated in distantly related hibernating bats and its expression level was higher in torpid bats than in active and non-hibernating bats (Fig 3), these results strongly suggest the adaptation of bat PPAR α to hibernation. The sizes of PPAR α detected in samples from *R. ferrumequinum* and *H. armiger* bats were slightly higher than expected (Fig 3A). This discrepancy may be due to variations in post-translational modifications (PTMs) of PPAR α as described previously [45]. The expression of PPAR α in mice was found to be higher than in all the hibernating and nonhibernating bats examined (Fig 3), suggesting a potential hibernation capability of mice. This possibility



is supported by the adenosine-induced torpid mice recently established by Swaop et al. [46].

In addition to using fat as the main energy source, bats maintain their blood glucose at 2–3 mM and catabolize amino acids to generate ketone bodies for energy supply during torpor [27]. PPARs are known to be involved in lipid metabolism and other cellular processes, such as insulin sensitivity, amino acid homeostasis, adaptation to starvation, and inflammation [31]. Overexpression of PPAR α activates nearly every gene associated with fatty acid catabolism [31]. Furthermore, *Ppara*-null mice exhibit increased glucose utilization, diminished fatty acid oxidation [15], and elevated expressions of many genes (e.g., arginase, phenylalanine hydroxylase, and spermidine synthetase) involved in amino acid metabolism [47]. Since hibernating mammals progressively suppress glucose utilization and use fat as the primary fuel [2], it is conceivable that bats produce sufficient amounts of PPAR α to meet their metabolic requirements during torpor. Previous studies indicated that PPAR α homeostasis is regulated by heterodimerization, recruitment of cofactors, post-translational modifications, and micro-RNAs (e.g., miR-519d) [48, 49]. Such regulation and the possible cross-talk among the various transcription factors observed in this study agree with the

notion that transcriptional or translational reprogramming of genes occurs during mammalian hibernation [40].

Variation of amino acid sequences of PPAR α in bats

To investigate the adaptation of PPAR α to hibernation, we compared the amino acid sequences of PPAR α from 9 hibernating and 3 non-hibernating species of bats. The human PPAR α sequence was used as the template. In the aligned region (amino acid positions 87 to 446), 316 amino acid sites were identical (87.78 %) and 44 amino acid sites were variable (see Additional file 3: Fig S3).

5 positions including V90, Y155, I195, T200, and I382 of PPAR α were conserved in hibernating bats but were different or divergent among non-hibernating bats. 38 amino acid sites of PPAR α were conserved in non-hibernating bats but were different among hibernating bats. Missense mutations at V90 and Y155 of PPAR α had been reported in carcinomas of the large intestine and liver, respectively [50], and missense mutation at G96 had been observed in malignant melanoma [50]. The amino acid site 155 is located in the zinc-finger motif (C4 degenerated type, CX₂CX₁₃CX₂CX_{14–15}CX₅CX₉CX₂C) of PPAR α (see Additional file 3: Fig S3). These results suggest the important role of these conserved amino acid sites in PPAR α . Taken together, these data agree with the conservation and functional constraint of PPAR α toward evolution (Fig 1 and Additional file 3: Fig S3).

Potential PPAR α Target genes

Genome-wide bioinformatic analyses were performed to estimate the mean ratio of the number of PPAR α potential target genes to the number of all annotated genes (see Additional file 1: Table S6) in bats and to calculate the mean affinity score of PPAR α to its target genes. 4 species of hibernating bats *Myotis brandtii*, *Myotis davidii*, *Myotis lucifugus*, and *Eptesicus fuscus* were found to have a higher mean target gene ratio than non-hibernating *Pteropus vampyrus* bats (see Additional file 3: Fig S4A), and the mean affinity score of PPAR α to its target genes of these hibernating bats was higher than that of non-hibernating bats, *Pteropus vampyrus* and *Pteropus alecto* (see Additional file 3: Fig S4B). These results imply that mammalian hibernators have more PPAR α target genes than non-hibernators and that PPAR α has a higher binding affinity to its target genes in hibernators than in non-hibernators. To test these possibilities, the mean ratio of the number of PPAR α potential target genes to the number of all genes in each of the 16 hibernating species and 48 non-hibernating species of mammals was determined; the mean affinity score of PPAR α to its target genes in each of these mammalian species was also calculated. Results showed that the mean target gene ratio of the hibernators

was significantly higher than that of the non-hibernators at a P value threshold of 5×10^{-7} (Fig 4A). This result was consistent across different settings of threshold P values (see Additional file 3: Fig S5 and Additional file 4). The mean affinity score of PPAR α to its target genes in the hibernators was 9.68 ± 0.24 , which is significantly higher than the score 9.37 ± 0.21 of the non-hibernators (Fig 4B and Additional file 1: Table S6). These data showed that hibernating mammals have more PPAR α target genes and that PPAR α has a higher affinity to its target genes in hibernating than in non-hibernating mammals.

To investigate phylogenetic inferences [51], we constructed a phylogenetic tree of 64 mammals (see Additional file 3: Fig S6A). The correlation between mammalian hibernation and the target gene ratio, or affinity score of PPAR α , was analyzed by 2 different phylogenetic comparative methods, including the quantitative genetic threshold model proposed by Felsenstein [52] and the phylogenetic ANOVA proposed by Garland et al. [53] (see Additional file 2). With both approaches, we found that the correlation between hibernation and affinity score of PPAR α was significant (95 % confidence interval 0.198 to 0.261; $P < 0.002$; see Additional file 1: Table S7). The correlation between hibernation and target gene ratio of PPAR α was also significant (P value threshold 5×10^{-7}) (see Additional file 1: Table S7 and Additional file 3: Fig S6B). However, the correlation coefficients were substantially decreased if the phylogeny of these mammals was considered. Therefore, phylogenesis is an important factor in the analysis of evolutionary adaptation of mammalian hibernation.

Differential gene expression plays a key role in the evolution of morphological phenotypes and some biological traits [54]. The evolution of phenotypic fitness is influenced, in part, by the divergent pattern of TF binding sites and different affinities of TFs to their binding sites. The crosstalk among TFs regulates transcription, ultimately leading to the complex phenotypes [54, 55]. It has been shown that TF binding sites evolve rapidly in

order to adapt to metabolic control and detoxification in the liver [56]. Our observations of more PPAR α target genes and a higher binding affinity of PPAR α to its target genes in hibernating mammals suggest an important regulatory role of PPAR α in hibernation. It is probable that the genomes of hibernators have evolved to adapt to hibernation.

Mammalian hibernation is an ideal model to investigate the role of differential gene expression in adaptive evolution [57]. The coding regions of most differentially expressed genes are shaped by purifying selection [54]. A recent comparative genomic study of 3 hibernating and several non-hibernating species of mammals found no signs of positive selection on the coding regions of genes associated with hibernation [58]. However, differential expression of genes of metabolic pathways commonly shared by 4 hibernating species (*Myotis brandtii*, *Ursus americanus*, *Spermophilus parryii*, and *Spermophilus tridecemlineatus*) was found, indicating the pivotal role of regulation of gene expression in mammalian hibernation [57, 58]. Our findings together with previous reports [58] suggest that both genomic information (e.g., gene sequences) and genomic processes (e.g., transcription and translation) of *Ppar α* have evolved toward adaptation to hibernation. More comparative studies of TF binding between torpid and active mammals or between hibernating and non-hibernating species will allow us to gain further insights into the evolution of mammalian hibernation.

Conclusions

In this study, we found PPAR α upregulation at both mRNA and protein levels in bat liver during torpor, providing clear evidence of PPAR α in adaptation to mammalian hibernation. Mechanisms by which bats upregulate the transcription and translation of PPAR α to achieve a torpid phenotype remain to be investigated. A complex crosstalk among different TFs, such as FOXL1, NFYA,

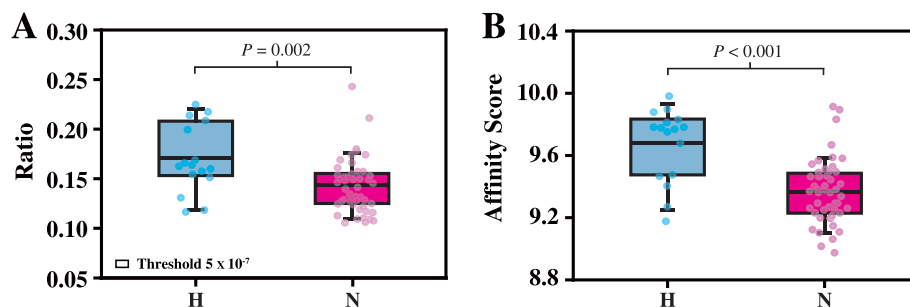


Fig. 4 Bioinformatic analyses of PPAR α in mammals. The y-axis in **(A)** represents the ratios of the number of PPAR α potential target genes to the number of all genes of different animals. The small open rectangle indicates the threshold setting (5×10^{-7}) for the matrix scan. The scores in **(B)** indicate the binding affinity of PPAR α to its target genes in different animals. Blue and pink boxes indicate data calculated from 16 hibernating species (H) and 48 non-hibernating species (N) of mammals. Each dot represents the mean value obtained from each mammalian species. The box plot shows the median, 25/75 percentiles (box), and 10/90 percentiles (bars). A P value < 0.05 is considered significant

NFYB, SP1, TBP, ERG, RELA, and E2F1, may be involved in the control of PPAR α expression. Results of evolutionary analyses and amino acid sequence alignments indicated that PPAR α is highly conserved among hibernators. Bioinformatic analyses revealed that the genomes of mammalian hibernators have evolved to become more susceptible to PPAR α regulation.

Methods

Animals and tissue acquisition

Acquisition of bats and experiments involving animals were done in accordance with ethical principles of the Animal Ethics Committee, East China Normal University (approval number AR2012/03001). 6 males each of the following hibernating bat species were captured from various locations in China: *Rhinolophus ferrumequinum* from Guan Ma Karst Cave (40°08'N, 126°05'E) in Jilin Province; *Hipposideros armiger* from Fish Cave (30°20'N, 117°50'E) in Anhui Province; *Myotis ricketti* from 7 Star Cave (25°16'N, 110°18'E) in Guangxi Province; *Taphozous melanopogon* from Ladian County (24°41'N, 108°01'E) in Guangxi Province; *Scotophilus heathii* from Mengla County (21°27'N, 101°33'E) in Yunnan Province; and *Ia io* from Feilong Cave (24°58'N, 104°53'E) in Guizhou Province (see Additional file 3: Fig 1). 3 bats of each species were sacrificed on site while they were in torpor, and the remaining bats were sacrificed 48hr after arousal from torpor in the laboratory. Rectal temperatures were approximately 8-10 °C for torpid and 36-37 °C for active bats. 3 males each of non-hibernating bat species *Rousettus leschenaultii*, *Cynopterus sphinx*, and *Eonycteris spelaea* were captured from Mashan County (23°55'N, 108°26'E) in Guangxi Province, Haikou Park (20°02'N, 110°20'E) in Hainan Province, and Xishuangbanna (22°0'N, 100°47'E) in Yunnan Province, China, respectively. Non-hibernating bats captured were sacrificed in the field. Mice were purchased from Sino-British Sippr/BK Lab Animal Ltd (Shanghai, China). These animals were sacrificed by cervical dislocation, and their liver tissues were rapidly excised, snap frozen in liquid nitrogen, and then stored in a -80 °C freezer until used.

RNA Isolation, cloning, and sequencing

Total RNA was isolated from the liver tissues using Trizol[®] reagent (Invitrogen, USA). A total of 5 μ g RNA was reverse transcribed to cDNA using the SuperScript[®] III Reverse Transcriptase kit (Invitrogen, USA). Primer pairs listed in Table 2 were used to amplify the coding region of bat *Ppara*. PCRs were carried out under the following conditions: denaturation at 95 °C for 5 min; 32 cycles of 95 °C for 30 s, 50 - 60 °C for 30 s, and 72 °C for 2 min; and a final extension at 72 °C for 10 min. The resulting DNA fragments were isolated by electrophoresis in 1 %

agarose gel and then ligated into pGEM[®]-T Easy Vector (Promega, USA). Recombinant plasmids were transformed into *E. coli* strain TOP10 (Tiangen, China). Bacterial colonies were screened by blue-white selection, and white colonies were picked for colony PCR. 6 positive clones of each PCR product were sequenced on an ABI 3730 DNA sequencer. All sequences obtained were submitted to GenBank (see Additional file 1: Table S8).

Sources of *Ppara* nucleotide sequences

Nucleotide sequences of *Ppara* were obtained from the following: 56 mammalian species of Placentalia and Marsupialia [59] (see Additional file 1: Table S8 and Additional file 3: Fig S2); 5 species of Yinpterochiroptera bats including 3 non-hibernating bat species (family Pteropodidae) *C. sphinx*, *E. spelaea*, and *R. leschenaultii* and 2 hibernating bat species *R. ferrumequinum* (family Rhinolophidae) and *H. armiger* (family Hipposideridae); and 7 species of hibernating Yangochiroptera bats including *T. melanopogon* (family Emballonuridae) and 6 species of family Vespertilionidae: *S. heathii*, *I. io*, *E. fuscus*, *M. ricketti*, *M. brandtii*, and *M. davidii*. These bats were chosen because their hibernation behaviors are known [9, 12]. The DNA sequences of *Ppara* of *E. fuscus*, *M. brandtii*, *M. davidii* and non-bat mammals, such as *Homo sapiens* and *Mus musculus*, were downloaded from GenBank.

Evolutionary analysis of *Ppara* of bats

The nucleotide sequences of *Ppara* were aligned using the software Clustal X [60]. DNA sequences were translated into amino acid sequences using the software MEGA5 [61]. The program CODEML in PAML (version 4.8) was used to estimate the ω value, which is derived from d_N (nonsynonymous substitution rate) divided by d_S (synonymous substitution rate). Species topology was constructed as previously described (Fig 1) [6, 62]. An ω value of 1, < 1, or > 1 represents neutral evolution, negative purifying selection, and positive selection, respectively. The one-ratio model analysis, which assumes an equal ω value among all branches, was first conducted to establish the null hypothesis [63]. The free ratio model, which allows ω values to vary among branches, was used to compare with the one-ratio model to test the heterogeneity of ω across the tree. The two-ratio model, which allows ω values to vary between the labeled and other branches, was also applied to each of the ancestral branches of 2 clades of hibernating bats from Yinpterochiroptera and Yangochiroptera (Table 1).

Real-time PCR

Total RNA was extracted from the liver tissues of hibernating bats *H. armiger*, *R. ferrumequinum*, and *M. ricketti*. 6 bats of each species were used, including 3 active

Table 2 Primers for cloning of bat *Ppara*

| Name | Sequences | Amplified species | Primer used | Product length (bp) | Length proportion |
|-------------------|---------------------------|-------------------------|-------------|---------------------|-------------------|
| <i>Ppara</i> -1 F | 5'-CTTGAGGCTGATGAYCTGGAAA | <i>E. spelaea</i> | 1 and 2 | 1361 | 96.73 % |
| <i>Ppara</i> -1R | 5'-TYGGGAAGAGGAAGRTGTCG | <i>R. leschenaultii</i> | 1 and 2 | 1361 | 96.73 % |
| <i>Ppara</i> -2 F | 5'-CAAYCCACCTTTYGTCAT | <i>C. sphinx</i> | 1 and 2 | 1361 | 96.73 % |
| <i>Ppara</i> -2R | 5'-ATRTCCCTGTAGATYCCT | <i>R. ferrumequinum</i> | 1 and 3 | 1362 | 96.80 % |
| <i>Ppara</i> -3 F | 5'-TGAATAAAGACGGGATGCT | <i>H. armiger</i> | 1 and 3 | 1362 | 96.80 % |
| <i>Ppara</i> -3R | 5'-CATGTCCTCTGTAGATTCCT | <i>T. melanopogon</i> | 4 | 1118 | 79.46 % |
| <i>Ppara</i> -4 F | 5'-CGGTGTCTTACCCTGTGGT | <i>S. heathii</i> | 4 | 1118 | 79.46 % |
| <i>Ppara</i> -4R | 5'-CGCCTCGTCTCTTGAT | <i>M. ricketti</i> | 4 | 1118 | 79.46 % |
| | | <i>I. io</i> | 4 | 1118 | 79.46 % |

and 3 torpid bats. The mRNA was reverse transcribed into cDNA as described above. The primer pairs used are listed in Table 3. 100 nanogram of cDNA was used to determine the expression level of *Ppara*. Real-time PCR was performed on an ABI Prism 7300 real-time PCR system (Applied Biosystems, UK) using the SYBR® *Premix Ex Taq*TM (Tli RNaseH Plus) kit (Takara, Japan). The $2^{-\Delta\Delta CT}$ method was applied to normalize the level of *Ppara* to that of *Gapdh* and to calculate the relative expression levels of *Ppara* between torpid and active bats [64-68].

Western blotting

Liver tissues (100 mg) from bats and mice were homogenized separately in 2-ml Eppendorf tubes, each containing 1.7 ml of lysis buffer (10 % glycerol, 2 % SDS, 1.25 % β -mercaptoethanol, 25 mM Tris-HCl, pH 6.8) and ceramic beads (0.17 g, 1 mm in diameter), using a Precellys® 24 grinder (Bertin Technologies, France) at 4 °C. The homogenates were centrifuged at 13,400 xg for 10 min at 4 °C. Supernatants were boiled at 100 °C for 10 min and then centrifuged at 13,400 xg for 10 min at 4 °C to remove insoluble cell debris. Each of the clarified supernatants was divided into small aliquots and stored at -80 °C until used. Protein concentration of each sample was determined

Table 3 Primers used in RT-PCR

| Genes and bat species | Primers ^a |
|---|---|
| <i>Ppara</i> and <i>M. ricketti</i> | F: 5'-AAAGCGAAACTGAAAGCAGAAATCC R: 5'-TCATGTTGAAGCTCCGACAGGTAG |
| <i>Ppara</i> and <i>R. ferrumequinum</i> | F: 5'-AGCCAACAACAATCCACCTTT R: 5'-AGCTCCGTGACAGTCTCCACA |
| <i>Ppara</i> and <i>H. armiger</i> | F: 5'-TTTCACAAGTGCCTTTCGGTTGG R: 5'-GATTTGAGGTCCGCCGTTTCG |
| <i>Gapdh</i> (internal control for all bat species) | F: 5'-ATGGGTGTGAACCAYGASAAGT R: 5'-GGTCATGAGTCCYTCCACRAT |

^aY = C + T, S = G + C, R = A + G.

using the Quick StartTM Bradford protein assay kit (Bio-Rad, USA) according to manufacturer's instructions.

Equal amount of each protein sample (20 μ g/lane) was subjected to a 12.5 % SDS-PAGE, and the separated proteins were transferred onto a PVDF membrane (Millipore, USA). The membrane was immersed in blocking buffer (5 % skim milk and 1 % BSA) at 4 °C overnight, and then probed with anti-PPAR α (1:100 dilution, Santa Cruz®, USA, sc-9000), which is a rabbit polyclonal antibody against a conserved N-terminal epitope of PPAR α . After washing with TBST buffer, the blot was reacted with an HRP-conjugated secondary antibody (Santa Cruz®, CA) at room temperature for 2 hours, followed by incubation with ImmobilonTM Western HRP Substrate Reagent (Millipore, USA). A reversible Ponceau S staining of the membrane was carried out to estimate the relative amount of each protein on the membrane [69]. Band intensity on the blot was quantified by the ImageQuantTM TL software (version 7.0, Amersham Biosciences), and the intensity of each band was normalized to the relative value of the corresponding Ponceau-stained protein band.

Bioinformatic Analyses of Target Genes and Determination of Affinity Scores of PPAR α

The ChIP-seq data derived from chromatin immunoprecipitation (ChIP) of human hepatoma cells with anti-PPAR α antibody were obtained from the GEO database (GSM864671) [36] and mapped to the mouse genome sequence (version mm9) [70]. The number of ChIP-seq peaks located in introns, exons, upstream regions of TSS (transcription start site), downstream regions of TTS, and other regions of all annotated genes in the mouse genome was separately calculated and divided by the total peak number to obtain the peak ratio of a particular location in the genome (see Additional file 3: Fig S7). A PPAR α target gene was defined if at least one binding site was located within introns, exons, or 10 kb upstream of TSS of the gene.

The nucleotide sequences of 10 kb upstream of TSS, introns, and exons of all annotated genes of each of the

64 mammalian species (see Additional file 1: Table S6) were retrieved from NCBI, Ensembl, or GigaDB [71]. The position frequency matrix (PFM) of PPAR α (f2) (see Additional file 3: Fig S8), which represents DNA sequence patterns recognized by PPAR α , was obtained from HOCOMOCO [72]. The matrix scan was first applied to estimate the number of putative binding sites of PPAR α in these sequences using parameters ‘-pseudo 1 -decimals 1 -2str -origin end -bg_pseudo 0.01 -return limits -return pval -uth pval 0.0000005’ [73]. The number of PPAR α target and non-target genes of each species was calculated based on the results of matrix scan. The ratio of PPAR α target gene was derived from the number of target genes divided by that of total genes (see Additional file 4). The downloaded sequences were scanned by f2 PMF using a modified SPeaker algorithm [74] to calculate the affinity score of PPAR α binding to each target gene. Only the highest score estimated for a gene was adopted. Results were analyzed by two-tailed Student’s *t*-test. A *P* value < 0.05 was considered significant.

To correlate the mammalian hibernation trait with the ratio of PPAR α target gene or PPAR α affinity to its target genes, 2 different phylogenetic comparison methods, including the quantitative genetic threshold model [52] and the phylogenetic ANOVA [53] were used (see Additional file 1: Table S7, Additional file 2, and Additional file 3: Fig S6). The phylANOVA and threshBayes in the R package phytools were conducted separately to determine the correlations [75].

Availability of supporting data

The data sets supporting the results of this article are available in the Dryad digital repository, [<http://dx.doi.org/10.5061/dryad.h6r74>] [76] DOI:10.5061/dryad.h6r74%5d%20%5b76. Gene sequences obtained in this study have been deposited in GenBank [<http://www.ncbi.nlm.nih.gov/genbank>]. Accession numbers are provided in Additional file 1.

Additional files

Below is the link to the electronic supplementary material.

Additional file 1: Table S1. Branch-site model A test for detection of positively selected sites in ancestral branches of hibernating bats. Table S2. Site model comparisons of 12 bat species. Table S3. Branch model tests of *Ppara* in 56 mammalian species. Table S4. Site model comparisons of 25 mammals. Table S5. Prediction of transcription factor binding to 3 potential regulatory regions (TSS_Around, TSS_Up, and TSS_Body) of *Ppara*. Table S6. Affinity scores of PPAR α binding to all annotated genes in 64 mammalian species. Table S7. Phylogenetic comparative methods for determining correlations among traits. Table S8. Accession numbers of *Ppara* sequences of 56 mammals.

Additional file 2: Supplementary methods for evolutionary analyses of *Ppara* in mammals and analyses of the binding affinity of each of the 205 transcription factors to the 3 potential regulatory regions of *Ppara* in various mammalian species.

Additional file 3: Figure S1. Geographical locations of bats obtained in China. The degrees of latitude and longitude are shown. Non-hibernating bats in Yinpterochiroptera, hibernating bats in Yinpterochiroptera, and hibernating bats in Yangochiroptera are represented by orange, green, and blue colors, respectively. Figure S2. Red dots A, B, C, and D denote the ancestral branch of Chiroptera; Cetartiodactyla, Perissodactyla, and Carnivora in Laurasiatheria; Rodentia and Lagomorpha; Scandentia and Primates in Euarchontoglires, respectively. The $N^*d_{\text{v}}/S^*d_{\text{g}}/\omega$ values of A, B, C, and D are shown below the red dots. Abbreviations Af, Au, Am, and M represent Afrotheria, Australidelphia, Ameridelphia, and Marsupialia, respectively. Red asterisks indicate the species that can hibernate. Figure S3. Amino acid sequence alignments of PPAR α of bats. Amino acid sequences of non-hibernating and hibernating bat species are denoted with pink and blue colors, respectively. The amino acid positions that are conserved in non-hibernating species but different or diverged among hibernating species are indicated with orange triangles. Amino acid sites that are conserved in hibernating species but different or diverged among non-hibernating species are denoted with red triangles. The green line shows the location of the zinc-finger motif. Figure S4. (A) The ratio of the number of PPAR α potential target genes to that of all genes in bats. The small open rectangle indicates the threshold setting for the matrix scan. (B) Mean scores of binding affinity of PPAR α to its target genes in bats. Blue and pink dots represent the mean value calculated from hibernating and non-hibernating bats, respectively. Figure S5. The y-axis in (A) represents the ratios of the number of PPAR α potential target genes to the number of all genes of different animals. The small open rectangle indicates the threshold setting for the matrix scan. The scores in (B) indicate the binding affinity of PPAR α to its target genes in different animals. Blue and pink boxes indicate data calculated from 16 hibernating species (H) and 48 non-hibernating species (N) of mammals. Each dot represents the mean value obtained from each mammalian species. The box plot shows the median, 25/75 percentiles (box), 10/90 percentiles (bars). A *P* value < 0.05 is considered significant. Figure S6. (A) Phylogenetic tree constructed for 62 mammalian species. Hibernating species are colored in red. (B) Results of phylogenetic ANOVA. The y-axis denotes scores of binding affinity of PPAR α to its target genes. The box plot shows the median, 25/75 percentiles (box), and 10/90 percentiles (bars). A *P* value < 0.05 is considered significant. Figure S7. Mapping of PPAR α binding sites to the mouse genome. The y-axis denotes the number of PPAR α binding sites located in various regions of all annotated genes, including the sequences upstream of TSS (UpStream), 5' un-translated sequences (5'UTR), exons (Coding Exon), introns (Intron), 3' untranslated sequences (3'UTR), the sequences downstream of TSS (DownStream), and the distal sequences (>20 kb) (Distal_Region). The Arabic number shown on top of each bar indicates the ratio of the number of binding sites in the region to the number of all PPAR α binding sites. Figure S8. Position frequency matrix (PFM) of sequences recognized by PPAR α .

Additional file 4: Different threshold settings of *P* value for the matrix scan of PPAR α in mammals.

Abbreviations

PPAR α : Peroxisome proliferator-activated receptor alpha; RXR: Retinoid X receptor; TFs: Transcription factors; FOXL1: Forkhead box protein L1; NFYA: Nuclear transcription factor Y subunit alpha; NFYB: Nuclear transcription factor Y subunit beta SP1, Specificity protein 1; TBP: TATA-box-binding protein 1; ERG: E-26 related gene; RELA: v-rel avian reticuloendotheliosis viral oncogene homolog A; E2F1: E2 Transcription Factor 1.

Competing interests

The authors declare that they have no competing interests.

Authors' contributions

YH and GZ carried out evolutionary analyses, performed biochemical experiments, and wrote the manuscript. YP designed the experiments and edited the manuscript. TY and DD performed bioinformatic analyses. YP and SZ provided experimental materials. All authors have read and approved the final manuscript.

Acknowledgements

We thank Tengting Zhu, Guangjian Zhu, and Junpeng Zhang for tissue collections, Tao Fang and Bin Shen for helpful comments on molecular evolutionary analyses, and Yang Liu for the discussions on phylogenetic analyses. We thank Dr. Chao-Hung Lee and Professor John F. Atkins for editing the manuscript and providing valuable advices. This work was supported by grants from the National Science Foundation of China (No. 31100273/C030101) to Yi-Hsuan Pan, Science and Technology Committee of Shanghai (No. 11XD1402000) and National Science Foundation of China (No. 31172077) to Shuyi Zhang.

Author details

¹Laboratory of Molecular Ecology and Evolution, Institute for Advanced Studies in Multidisciplinary Science and Technology, East China Normal University, Shanghai 200062, China. ²State Key Laboratory of Estuarine and Coastal Research, East China Normal University, Shanghai 200062, China. ³Laboratory of Molecular Ecology and Evolution, Institute of Estuarine and Coastal Research, East China Normal University, Shanghai 200062, China.

Received: 1 September 2014 Accepted: 29 April 2015

Published online: 17 May 2015

References

- Geiser F. Hibernation. *Current Biology*. 2013;23(5):R188–93.
- Carey HV, Andrews MT, Martin SL. Mammalian hibernation: cellular and molecular responses to depressed metabolism and low temperature. *Physiol Rev*. 2003;83(4):1153–81.
- Storey KB, Storey JM. Metabolic rate depression: the biochemistry of mammalian hibernation. *Advances in clinical chemistry*. 2010;52:78.
- Andrews MT. Advances in molecular biology of hibernation in mammals. *Bioessays*. 2007;29(5):431–40.
- Lyman C. Termoregulation and metabolism in bats. In: Wimsatt W, editor. *In Biology of bats*. New York: Academic; 1970. p. 301–30.
- Teeling EC, Springer MS, Madsen O, Bates P, O'Brien SJ, Murphy WJ. A molecular phylogeny for bats illuminates biogeography and the fossil record. *Science*. 2005;307(5709):580–4.
- Simmons N. Order Chiroptera. In: DM WDR, editor. *Mammal species of the world: a taxonomic and geographic reference*. Baltimore, Maryland: Johns Hopkins University Press; 2005. p. 312–529.
- Geiser F, Stawski C. Hibernation and torpor in tropical and subtropical bats in relation to energetics, extinctions, and the evolution of endothermy. *Integrative and comparative biology*. 2011;51(3):337–48.
- Ransome R. The Natural History of Hibernating Bats. In *The Natural History of Hibernating Bats*. London: Christopher Helm: Academic Press Inc; 1990.
- Lyman CP. Hibernation and torpor in mammals and birds: Elsevier. 2013.
- Zhang G, Cowled C, Shi Z, Huang Z, Bishop-Lilly KA, Fang X, et al. Comparative analysis of bat genomes provides insight into the evolution of flight and immunity. *Science*. 2013;339(6118):456–60.
- Yuan L, Zhao X, Lin B, Rossiter SJ, He L, Zuo X, et al. Adaptive evolution of Leptin in heterothermic bats. *PLoS one*. 2011;6(11), e27189.
- Dreyer C, Krey G, Keller H, Givel F, Helftenbein G, Wahli W. Control of the peroxisomal β -oxidation pathway by a novel family of nuclear hormone receptors. *Cell*. 1992;68(5):879–87.
- Feige JN, Gelman L, Michalik L, Desvergne B, Wahli W. From molecular action to physiological outputs: peroxisome proliferator-activated receptors are nuclear receptors at the crossroads of key cellular functions. *Progress in lipid research*. 2006;45(2):120–59.
- Bernal-Mizrachi C, Weng S, Feng C, Finck BN, Knutsen RH, Leone TC, et al. Dexamethasone induction of hypertension and diabetes is PPAR- α dependent in LDL receptor-null mice. *Nature medicine*. 2003;9(8):1069–75.
- Tan NS, Michalik L, Desvergne B, Wahli W. Multiple expression control mechanisms of peroxisome proliferator-activated receptors and their target genes. *The Journal of steroid biochemistry and molecular biology*. 2005;93(2):99–105.
- Nelson CJ, Otis JP, Carey HV. A role for nuclear receptors in mammalian hibernation. *The Journal of physiology*. 2009;587(9):1863–70.
- Desvergne B, Michalik L, Wahli W. Transcriptional regulation of metabolism. *Physiol Rev*. 2006;86(2):465–514.
- Berger J, Moller DE. The mechanisms of action of PPARs. *Annual review of medicine*. 2002;53(1):409–35.
- Inagaki T, Dutchak P, Zhao G, Ding X, Gautron L, Parameswara V, et al. Endocrine regulation of the fasting response by PPAR α -mediated induction of fibroblast growth factor 21. *Cell metabolism*. 2007;5(6):415–25.
- Xu Y, Shao C, Fedorov VB, Goropashnaya AV, Barnes BM, Yan J. Molecular signatures of mammalian hibernation: comparisons with alternative phenotypes. *BMC genomics*. 2013;14(1):567.
- Lin B, Yuan L, Chen J. Selection pressure drives the co-evolution of several lipid metabolism genes in mammals. *Chinese Science Bulletin*. 2012;57(8):877–85.
- Eddy SF, Morin Jr P, Storey KB. Cloning and expression of PPAR γ and PGC-1 α from the hibernating ground squirrel, *Spermophilus tridecemlineatus*. *Molecular and cellular biochemistry*. 2005;269(1):175–82.
- Eddy SF, Storey KB. Differential expression of Akt, PPAR γ , and PGC-1 during hibernation in bats. *Biochemistry and cell biology*. 2003;81(4):269–74.
- Kabine M, El Kebbab Z, Oaxaca-Castillo D, Clémencet M-C, Latruffe N, Cherkaoui-Malki M. Peroxisome proliferator-activated receptors as regulators of lipid metabolism; tissue differential expression in adipose tissues during cold acclimatization and hibernation of jerboa (*Jaculus orientalis*). *Biochimie*. 2004;86(11):763–70.
- El Kebbab Z, Andreoletti P, Mountassif D, Kabine M, Schohn H, Dauça M, et al. Differential regulation of peroxisome proliferator-activated receptor (PPAR)- α 1 and truncated PPAR α 2 as an adaptive response to fasting in the control of hepatic peroxisomal fatty acid β -oxidation in the hibernating mamma. *Endocrinology*. 2009;150(3):1192–201.
- Pan YH, Zhang Y, Cui J, Liu Y, McAllan BM, Liao CC, et al. Adaptation of phenylalanine and tyrosine catabolic pathway to hibernation in bats. *PLoS one*. 2013;8(4), e62039.
- Melvin RG, Andrews MT. Torpor induction in mammals: recent discoveries fueling new ideas. *Trends in Endocrinology & Metabolism*. 2009;20(10):490–8.
- Yaqoob P. Fatty acids as gatekeepers of immune cell regulation. *Trends in immunology*. 2003;24(12):639–45.
- Hotamisligil GS. Inflammation and metabolic disorders. *Nature*. 2006;444(7121):860–7.
- Wahli W, Michalik L. PPARs at the crossroads of lipid signaling and inflammation. *Trends in Endocrinology & Metabolism*. 2012;23(7):351–63.
- Meijer AJ, Dubbelhuis PF. Amino acid signalling and the integration of metabolism. *Biochemical and biophysical research communications*. 2004;313(2):397–403.
- Katz JP, Perreault N, Goldstein BG, Chao H-H, Ferraris RP, Kaestner KH. Foxl1 null mice have abnormal intestinal epithelia, postnatal growth retardation, and defective intestinal glucose uptake. *American Journal of Physiology-Gastrointestinal and Liver Physiology*. 2004;287(4):G856–64.
- Reed BD, Charos AE, Szekely AM, Weissman SM, Snyder M. Genome-wide occupancy of SREBP1 and its partners NFY and SP1 reveals novel functional roles and combinatorial regulation of distinct classes of genes. *PLoS genetics*. 2008;4(7), e1000133.
- Clarke SD. Polyunsaturated fatty acid regulation of gene transcription: a molecular mechanism to improve the metabolic syndrome. *J Nutr*. 2001;131(4):1129–32.
- van der Meer DL, Degenhardt T, Väisänen S, de Groot PJ, Heinäniemi M, de Vries SC, Müller M, Carlberg C, Kersten S. Profiling of promoter occupancy by PPAR α in human hepatoma cells via ChIP-chip analysis. *Nucleic Acids Res* 2010;gkq012.
- Lim C-A, Yao F, Wong JJ-Y, George J, Xu H, Chiu KP, et al. Genome-wide mapping of RE1A (p65) binding identifies E2F1 as a transcriptional activator recruited by NF- κ B upon TLR4 activation. *Molecular cell*. 2007;27(4):622–35.
- Glass CK, Ogawa S. Combinatorial roles of nuclear receptors in inflammation and immunity. *Nature Reviews Immunology*. 2005;6(1):44–55.
- Doetzlhofer A, Rotheneder H, Lagger G, Koranda M, Kurtev V, Brosch G, et al. Histone deacetylase 1 can repress transcription by binding to Sp1. *Molecular and cellular biology*. 1999;19(8):5504–11.
- Morin Jr P, Storey KB. Mammalian hibernation: differential gene expression and novel application of epigenetic controls. *International Journal of Developmental Biology*. 2009;53(2):433.
- Carey H, Frank C, Seifert J. Hibernation induces oxidative stress and activation of NF- κ B in ground squirrel intestine. *Journal of Comparative Physiology B*. 2000;170(7):551–9.
- Allan ME, Storey KB. Expression of NF- κ B and downstream antioxidant genes in skeletal muscle of hibernating ground squirrels, *Spermophilus tridecemlineatus*. *Cell biochemistry and function*. 2012;30(2):166–74.

43. Eddy SF, McNally J, Storey K. Up-regulation of a thioredoxin peroxidase-like protein, proliferation-associated gene, in hibernating bats. *Archives of biochemistry and biophysics*. 2005;435(1):103–11.
44. Lim WS, Ng DL, Kor SB, Wong HK, Tengku-Muhammad TS, Choo QC, et al. Tumour necrosis factor alpha down-regulates the expression of peroxisome proliferator activated receptor alpha (PPAR α) in human hepatocarcinoma HepG2 cells by activation of NF- κ B pathway. *Cytokine*. 2013;61(1):266–74.
45. Wadosky KM, Willis MS. The story so far: post-translational regulation of peroxisome proliferator-activated receptors by ubiquitination and SUMOylation. *American Journal of Physiology-Heart and Circulatory Physiology*. 2012;302(3):H515–26.
46. Swoap SJ, Illiff B, Le S. Adenosine, AMP, and Daily Torpor. In: Thomas R, Claudia B, Walter A, Eva M, editors. *Living in a Seasonal World*. Springer. 2012. p. 337–49.
47. Kersten S, Mandard S, Escher P, Gonzalez FJ, Tafuri S, Desvergne B, et al. The peroxisome proliferator-activated receptor α regulates amino acid metabolism. *The FASEB Journal*. 2001;15(11):1971–8.
48. Blanquart C, Mansouri R, Fruchart J-C, Staels B, Glineur C. Different ways to regulate the PPAR α stability. *Biochemical and biophysical research communications*. 2004;319(2):663–70.
49. Martinelli R, Nardelli C, Pilone V, Buonomo T, Liguori R, Castanò I, et al. P: miR-519d overexpression is associated with human obesity. *Obesity*. 2010;18(11):2170–6.
50. Forbes SA, Bindal N, Bamford S, Cole C, Kok CY, Beare D, et al. COSMIC: mining complete cancer genomes in the Catalogue of Somatic Mutations in Cancer. *Nucleic Acids Res*. 2011;39(D1):D945–50.
51. Garland T, Bennett AF, Rezende EL. Phylogenetic approaches in comparative physiology. *Journal of experimental Biology*. 2005;208(16):3015–35.
52. Felsenstein J. A comparative method for both discrete and continuous characters using the threshold model. *The American Naturalist*. 2012;179(2):145–56.
53. Garland T, Dickerman AW, Janis CM, Jones JA. Phylogenetic analysis of covariance by computer simulation. *Systematic Biology*. 1993;42(3):265–92.
54. Romero IG, Ruvinsky I, Gilad Y. Comparative studies of gene expression and the evolution of gene regulation. *Nature Reviews Genetics*. 2012;13(7):505–16.
55. Wittkopp PJ, Haerum BK, Clark AG. Evolutionary changes in cis and trans gene regulation. *Nature*. 2004;430(6995):85–8.
56. Brawand D, Soumillon M, Necsulea A, Julien P, Csárdi G, Harrigan P, et al. The evolution of gene expression levels in mammalian organs. *Nature*. 2011;478(7369):343–8.
57. Srere HK, Wang L, Martin SL. Central role for differential gene expression in mammalian hibernation. *Proceedings of the National Academy of Sciences*. 1992;89(15):7119–23.
58. Villanueva-Cañas JL, Faherty SL, Yoder AD, Albà MM. Comparative Genomics of Mammalian Hibernators Using Gene Networks. *Integrative and Comparative Biology*. 2014;54(3):452–62.
59. Murphy WJ, Pevzner PA, O'Brien SJ. Mammalian phylogenomics comes of age. *Trends in Genetics*. 2004;20(12):631–9.
60. Thompson JD, Gibson T, Higgins DG. Multiple sequence alignment using ClustalW and ClustalX. *Current protocols in bioinformatics*. 2002;23(1–2):3–22.
61. Tamura K, Peterson D, Peterson N, Stecher G, Nei M, Kumar S. MEGA5: molecular evolutionary genetics analysis using maximum likelihood, evolutionary distance, and maximum parsimony methods. *Molecular biology and evolution*. 2011;28(10):2731–9.
62. Zhou X, Xu S, Xu J, Chen B, Zhou K, Yang G. Phylogenomic analysis resolves the interordinal relationships and rapid diversification of the Laurasiatherian mammals. *Systematic biology*. 2012;61(1):150–64.
63. Yang Z. PAML 4: phylogenetic analysis by maximum likelihood. *Molecular biology and evolution*. 2007;24(8):1586–91.
64. Livak KJ, Schmittgen TD. Analysis of Relative Gene Expression Data Using Real-Time Quantitative PCR and the $2^{-\Delta\Delta CT}$ Method. *methods*. 2001;25(4):402–8.
65. Schmittgen TD, Livak KJ. Analyzing real-time PCR data by the comparative CT method. *Nat Protoc*. 2008;3(6):1101–8.
66. Barber RD, Harner DW, Coleman RA, Clark BJ. GAPDH as a housekeeping gene: analysis of GAPDH mRNA expression in a panel of 72 human tissues. *Physiological genomics*. 2005;21(3):389–95.
67. Soukri A, Valverde F, Hafid N, Elkebbaj M, Serrano A. Occurrence of a differential expression of the glyceraldehyde-3-phosphate dehydrogenase gene in muscle and liver from euthermic and induced hibernating jerboa (*Jaculus orientalis*). *Gene*. 1996;181(1):139–45.
68. Vandesompele J, De Preter K, Pattyn F, Poppe B, Van Roy N, De Paepe A, Speleman F. Accurate normalization of real-time quantitative RT-PCR data by geometric averaging of multiple internal control genes. *Genome biology* 2002, 3(7):research0034
69. Romero-Calvo I, Ocón B, Martínez-Moya P, Suárez MD, Zarzuelo A, Martínez-Augustín O, et al. Reversible Ponceau staining as a loading control alternative to actin in Western blots. *Analytical biochemistry*. 2010;401(2):318–20.
70. Chinwalla AT, Cook LL, Delehaunty KD, Fewell GA, Fulton LA, Fulton RS, et al. Initial sequencing and comparative analysis of the mouse genome. *Nature*. 2002;420(6915):520–62.
71. Flicek P, Ahmed I, Amode MR, Barrell D, Beal K, Brent S, et al. Ensembl 2013. *Nucleic Acids Res*. 2012;41(D1):D48–55.
72. Kulakovskiy IV, Medvedeva YA, Schaefer U, Kasianov AS, Vorontsov IE, Bajic VB, et al. HOCOMOCO: a comprehensive collection of human transcription factor binding sites models. *Nucleic Acids Res*. 2013;41(D1):D195–202.
73. Thomas-Chollier M, Defrance M, Medina-Rivera A, Sand O, Herrmann C, Thieffry D, et al. RSAT 2011: regulatory sequence analysis tools. *Nucleic Acids Res*. 2011;39 suppl 2:W86–91.
74. Megraw M, Pereira F, Jensen ST, Ohler U, Hatzigeorgiou AG. A transcription factor affinity-based code for mammalian transcription initiation. *Genome research*. 2009;19(4):644–56.
75. Revell LJ. Phytools: an R package for phylogenetic comparative biology (and other things). *Methods in Ecology and Evolution*. 2012;3(2):217–23.
76. Han Y-J, Zheng G-T, Yang T-X, Zhang S-Y, Dong D, Pan Y-H. Supporting data for PPAR α and hibernation. In: Dryad Digital Repository. (2015. <http://dx.doi.org/10.5061/dryad.h6r74>).

Submit your next manuscript to BioMed Central and take full advantage of:

- Convenient online submission
- Thorough peer review
- No space constraints or color figure charges
- Immediate publication on acceptance
- Inclusion in PubMed, CAS, Scopus and Google Scholar
- Research which is freely available for redistribution

Submit your manuscript at
www.biomedcentral.com/submit

